RSC Advances

ROYAL SOCIETY OF CHEMISTRY

www.rsc.org/advances

Journal Name

COMMUNICATION

Engineered biomimetic nanoabsorbent for cellular detoxification of chemotherapeutics

Received 00th January 20xx,
Accepted 00th January 20xx

DOI: 10.1039/x0xx00000x

www.rsc.org/

Tuyen Duong Thanh Nguyen,[a,b] Arunkumar Pitchaimani,[a,b,c] Mukund Bahadur Koirala,[a,b,c] Faqir Muhammad,[c,d] Santosh Aryal[a,b*]

An approach to reduce nonspecific cytotoxicity of chemotherapeutics have been put-forth using biomimetic nanoabsorbent (NAb) as a detoxifying agent. The engineered NAb possesses tunable drug absorption ability depending on the charge of the absorbing molecule, in which the cooperative absorption ability of core and shell significantly reduces the cellular toxicity.

Chemotherapy has been widely accepted and used as a clinical treatment for tumor management and has occupied a well-defined role in the prognosis of many hematological neoplasms and solid tumors.[1–3] Unfortunately, apart from cancerous cells, the large majority of chemotherapeutic agents also extravasate into the healthy cells resulting adverse side effects for example: inadvertent perivenous drug infiltrations with tissue damage, cardiomyopathy, ulcer formation, altered limb function, pain, and impact on the quality of life.[4–9] Nearly, 40% of toxic exposures in humans are associated with chemotherapeutic drug overdoses. However, there are limited detoxification treatment opportunities available in clinic. The common treatments for these types' intoxications are based on general intoxication measures such as administration of whole bowel irrigation,[10,11] correction of electrolyte disturbances,[12,13] and removal of toxin through extracorporeal procedures along with antidotes for a limited number of toxic agents.[14–17]

Owing to the limitations of aforementioned intoxication supports, alternate strategy for managing chemotherapy related toxicity involves injecting nanosized particulate carriers in the form of liposomes, nanoemulsions, nanoparticles, and macromolecules have gained increasing interest in recent years.[18–21] Such injected nanocarrier work in the way that they either travel in the circulatory system or have diffused in the peripheral organs to extract the drug from the intoxicated sites and then exit the body via the excretory system. These nanocarriers possess high specific surface area and tunable surface properties to optimize uptake and plasma residence time, which ensure the efficient removal of toxins from the circulatory system and peripheral tissues. Although these nanoparticle-assisted methods of detoxification have demonstrated the ability to capture target toxins, there are some drawbacks that limit their therapeutic applications. For example: the extraction with micro emulsions and ligand-based nanoparticles occurs through the adsorption of toxic molecules to the outer surface of the particle, recognition by immune system results in short blood circulation half-life, and the extraction efficiency is greatly reduced in vivo due to the presence of large amounts of serum proteins for which toxins have a high binding affinity.[22,23] The relation between the formation of a protein biocorona and the fate of nanoparticles in physiological environment have been extensively documented.[24–27] In the presence of these proteins, a nanodetoxifier changes its chemical and physical properties and must aggressively compete for the binding of toxic molecules. In addition, due to the low capture efficiency, a higher concentration of nanoparticles must be administered to reach the therapeutic levels of treatment.

[a] *Department of Chemistry, Kansas State University, Manhattan, KS 66506*
[b] *Nanotechnology Innovation Center of Kansas State (NICKS), Kansas State University, Manhattan, KS 66506*
[c] *Department of Anatomy and Physiology, Kansas State University, Manhattan, KS 66506.*
[d] *Institute of Pharmacy, Physiology and Pharmacology, University of Agriculture Faisalabad, Pakistan.*
* Corresponding author: Dr. Santosh Aryal, Email: saryal@ksu.edu.
Electronic Supplementary Information (ESI) available: [details of any supplementary information available should be included here]. See DOI: 10.1039/x0xx00000x

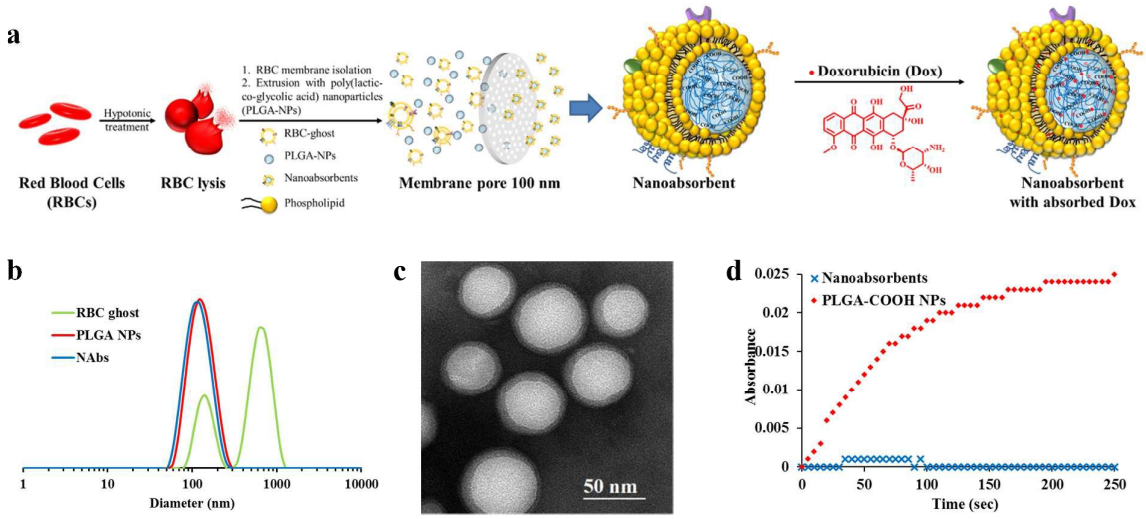

Fig. 1 Strategic fabrication and physiochemical properties of NAbs. (a) Schematic representation showing each steps of NAbs fabrication and absorption of doxorubicin. (b) Hydrodynamic size measurement of NAbs, PLG and RBC ghost particles using dynamic light scattering technique. (c) Transmission electron microscopic micrographs showing anatomical structure of core-shell NAbs. (d) Serum stability test measured spectrophotometrically at optical density of 560 nm using 100% serum.

Recently, red blood cell (RBC) membrane coated poly lactic-co-glycolic acid (PLGA-COOH) nanoparticles have been employed for toxin absorption and detainment in mice.[28] In which the PLGA core was used as a stabilizer for RBC membrane and toxins were absorbed onto the surface of nanoconstruct. In these studies, researchers have studied in detail the neutralization of bacterial toxin, staphylococcal alpha-haemolysin (α-Toxin), using mice model where the effect of toxin was significantly suppressed in both subcutaneous and systemic injection models. In addition to large molecule like α-Toxin, treatment of intoxication due to small molecule chemotherapeutics used in cancer treatment is of great interest to reduce off target toxicity. However, there is no any report regarding the possible absorption of small molecular chemotherapeutics, like DOX, in cellular microenvironment using biomimetic system that has a stealth property equivalent to that of RBC. Herein, attention has been given to the detoxification of small molecular chemotherapeutic using red blood cell membrane coated poly(lactic-co-glycolic acid) as a NAb and the role of polymeric core in absorption.

In this study, doxorubicin (DOX), an anthracycline antibiotic, was chosen as a drug of interest, as it has been widely used for various cancer treatment. However, the clinical application of DOX have been severely hindered because of its critical cardiotoxicity, narrow therapeutic window, and the development of multidrug resistance (MDR). Therefore, it is very important to eliminate excess of DOX or delay its cytotoxic effect in order to minimize adverse side effect which in turn significantly mitigate the biological effect of the sequestered drugs. Along with cationic DOX, we have also taken an anionic drug, Methotrexate (MTX), to understand in detail the absorption phenomenon of NAb.

Engineered Biomimetic NAb fabricated in this study is a construct made up of carboxylate terminated Poly(lactic-co-glycolic acid) (PLGA) core decorated with the bilayer membrane of red blood cells (RBCs) as a shell as demonstrated in Fig. 1. Since the engineering construct of proposed NAb is designed to mimic the surface properties of RBC, we called it as a Biomimetic NAb. Although the extensive work was done in this system, the PLGA core has only been exploited as a skeleton of the system. Less attention has been given to the additional possible role of the PLGA, such as a depot for absorbed toxin. Considering this outstanding possible role of PLGA, herein we have demonstrated the cellular chemotherapeutics detoxification potential of NAbs by taking DOX, as a positively charged drug, and MTX, as a negatively charged drug, in order to understand the effect of PLGA core.

PLGA is a well know polymer which exhibits properties like biocompatibility, biodegradability, and ability to encapsulate various types of drugs e.g. hydrophilic or hydrophobic small molecules or macromolecules. The United State Food and Drug Administration (FDA) have approved to use PLGA in various biomedical applications. Moreover, the hydrolysis of PLGA leads to metabolite monomers, lactic acid and glycolic acid, which are endogenous and easily metabolized by the body via the Krebs cycle. In addition, the carboxylate terminated PLGA nanoparticles are stable in aqueous condition that can be fused with RBC membrane as shown in Fig. 1 to fabricate NAbs.

NAbs were fabricated via extrusion technique using PLGA nanoparticles and the RBC membrane vesicles, in which vesicles were fused onto the surface of PLGA.[29,30,28] As show in Fig. 1b, dynamic light scattering technique was used to study the hydrodynamic diameter of the NAbs. The multimodal distribution of membrane vesicles becomes unimodal when stabilized onto the sub 100 nm PLGA nanoparticles. Both PLGA NPs and NAbs hydrodynamic diameter are nearly similar and there is no significant difference, which is probably due to the fact that small increase in size of PLGA NPs due to the bilayer

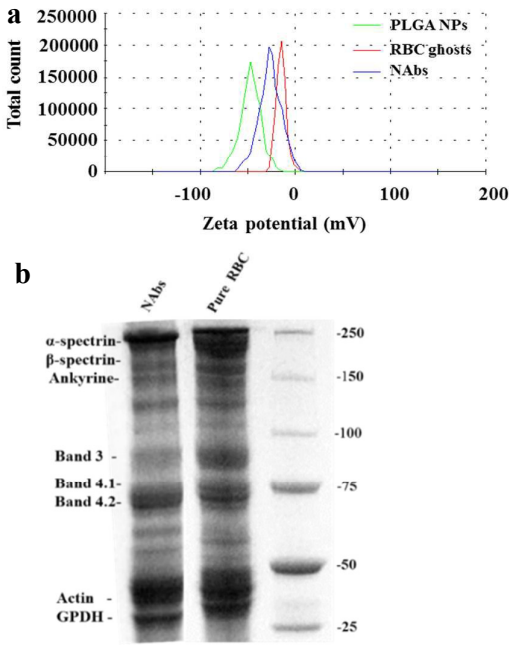

Fig. 2 Surface characteristics properties (a) zeta-potential measurements of NAbs, PLGA, and RBC ghost nanoparticles and (b) SDS PAGE electrophoresis to study the membrane protein retention after RBC membrane translocation into NAbs.

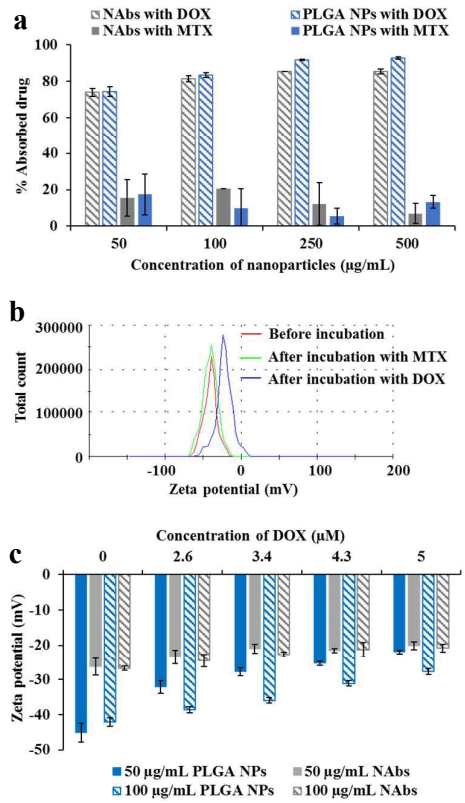

Fig. 3 Study of chemotherapeutics absorption into the NAbs. (a) Spectrophotometric determination of DOX and MTX absorption into the NAbs and PLGA NPs. (b) Variation in surface charge before and after drug absorption. (c) Changes in the surface charge of NAbs when treated with different concentration of DOX. Value represents mean ± s.d., n = 3.

of RBC membrane is difficult to distinguish under hydrodynamic condition. However, the PLGA core coated with membrane vesicles is clearly visible in the transmission electron micrographs (TEM) (Fig. 1c). TEM micrograph showed that NAbs are highly monodispersed and uniform core-shell in structure. Moreover, NAbs are found to be highly stable in serum as shown in Fig. 1d. Serum stability test examined in Fig. 1d is a simple absorbance test based on the particle aggregation under serum environment, which is the direct measure of particle aggregation at optical density (O.D.) 560 nm.[30]

With the assurances of hydrodynamic stability and anatomical structure of NAbs, we next examined the surface properties by measuring the surface charge and intactness of the RBC surface markers in NAbs. The zeta potential measurement tests were carried for PLGA NPs, NAbs, and RBC vesicles separately. It was found that PLGA NPs are highly charged with negative zeta potential of -50 mV and RBC vesicles are -20 mV. Upon fusion of RBC vesicles and PLGA NPs to form NAbs, the zeta potential is at the median range of -25 mV. Change in surface charge indicated the successful RBC membrane translocation and formation of NAbs. Furthermore, SDS-PAGE electrophoresis was conducted to find the fate of RBC surface markers and proteins in NAbs. As can be seen from the SDS-PAGE micrograph (Fig. 2b), the entire surface marker proteins of the RBCs were successfully translocated onto the surface of the NAbs, confirming that the prepared NAb holds surface retention properties of RBC. This further supports the claims observed in the zeta potential measurement and the TEM micrograph.

Fig. 3 explains the drug absorption ability of NAbs at varying concentrations. For the process four different concentrations of NAbs and PLGA NPs (50, 100, 250, and 500 µg/mL) were incubated with known amount of DOX and MTX, respectively. The amount of absorbed drug into the respective particles was quantified spectrophotometrically. As shown in Fig. 3a, both bare PLGA NPs and NAbs absorbed DOX in the same extents. Nearly, 80% of DOX was absorbed in both cases. However, absorption of MTX in both cases is minimum, which can be attributed to the negatively charged surface of bare PLGA NPs and NAbs. MTX is itself a negatively charged drug which most probably won't be absorbed on the negatively charged surfaces because of inherent electrostatic repulsion of same charges, this suggests that ionic repulsion is the major energy barrier for MTX not being absorbed. Furthermore, zeta-potential of PLGA NPs before (-45 mV) and after incubation of MTX was almost same (-46 mV) as shown in Fig. 3b, suggesting no significant interaction with PLGA NPs. In contrast, zeta potential of PLGA before and after DOX absorption was significantly varied from -46 mV to -21 mV. In fact, this change in zeta-potential broadly defines the interaction with PLGA NPs is charge dependent (note: DOX is cationic and MTX is anionic drug). The charge dependent nature of interaction further encouraged us to explore and understand the DOX absorption phenomenon, where DOX goes after absorption into the NAbs, whether it remains on the surface or pulled into the PLGA core. To answer these questions, an experiment with various concentrations of DOX (from 0 to 5 µM) was performed with

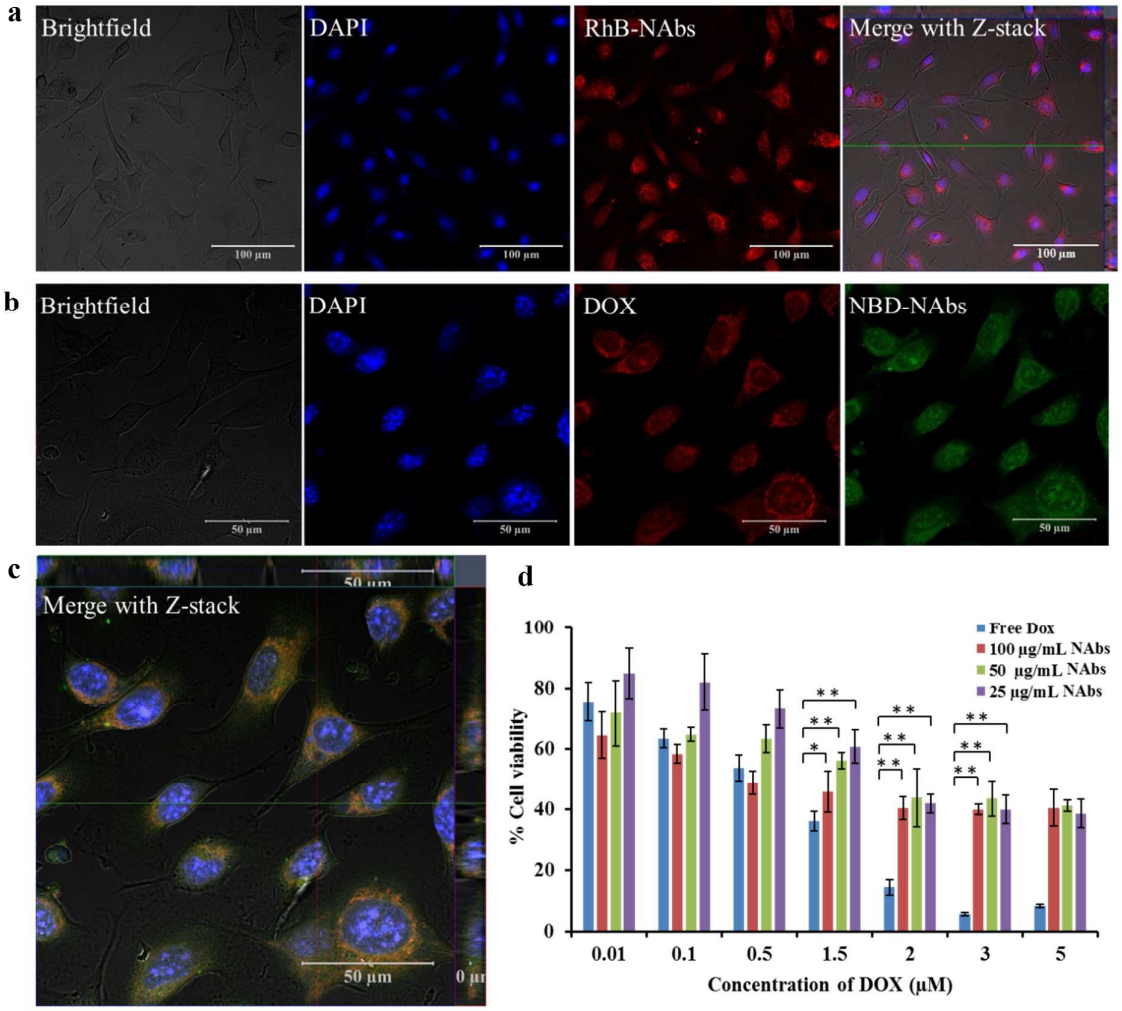

Fig 4. Cellular studies (a) Confocal microscopic micrographs at various field showing internalization of NAbs into the B16-F10 melanoma cells confirming the perinuclear colocalization of NAbs, (b) study of Intracellular structural integrity of NAbs by labelling core and shell with red (DOX) and Green (lipid-NBD) fluorescent dyes, respectively, (c) Merge with Z-stack of micrographs in b and (d) cellular detoxification of DOX studies performed at variable concentrations of DOX and NAbs. Free DOX Study was performed in absence of NAbs. Represent mean ± s.d., n = 6. ($^{*}P< 0.01$,$^{**}P< 0.001$, Student's t-test)

two different concentrations of PLGA NPs and NAbs as shown in Fig. 3C. Significant change (-46 mV to -21 mV) in surface charge was observed when bare PLGA NPs were incubated with different DOX concentrations. However, no significant change in surface charge of NAbs was observed when incubated with various concentration of DOX (Fig. 3c), this is only possible when surface absorbed DOX further electrostatically pulled to be buried into the negative PLGA core of NAbs. Therefore, PLGA herein not only act as a skeleton of the NAbs but also function as a depot of cationic drug like DOX. In addition to the drug absorption efficiency, the most important factor to be considered is the stability of nanoconstruct after absorbing drug. It was found that the bare PLGA NPs after DOX absorption immediately aggregated and pelleted down whereas NAb was well dispersed as nanosuspension. The observed phenomenon further confirmed that the NAb was well dispersed nanosuspension with uniform hydrodynamic size distribution; colloidal polydispersity index (PDI) at this stage was 0.09. Due to the promising chemotherapeutic absorption ability of NAb, our interest to understand its ability to detoxify cells was focused on DOX in our cellular studies.

The in vitro cellular detoxification of DOX was studied at various NAbs concentrations. First, the NAb cellular internalization study was conducted after labeling the RBC vesicles with lipid-rhodamine conjugate. The insertion of lipid-rhodamine into the RBC vesicles and subsequent fabrication of NAbs makes it an integral part of nanoconstruct. Fig. 4a demonstrated that the cellular internalization of NAbs had taken place and localized into the cellular microenvironment. The merged confocal micrographs of brightfield, DAPI, and RhB with Z-stack clearly showed the perinuclear colocalization of NAbs. Moreover, the structural integrity of NAbs was assayed by labelling core and shell of NAbs with different color dyes. In typical experiment, absorbed DOX into the core of NAbs was taken advantage to label the core and the shell was labeled via insertion of lipid-NBD green dye. As can be seen from Fig. 4b & c, both red and green fluorescent co-localized to produce

orange yellow color. The merged z-stack confocal micrograph (Fig. 4c) approves that the structure of NAbs was intact during the internalization process which further confirms the ability to hold DOX in PLGA core. In addition, over the wide range of NAbs concentration, no significant toxicity related to NAbs was observed (supporting information Fig. 1). Understanding the cellular internalization and compatibility of NAbs, cellular detoxification of DOX was studied using B16-F10 melanoma cells as a model cell. In a typical experiment, cells were first treated with 100, 50, and 25 μg/mL concentration of NAbs and incubated for 4 hrs. After 4 hrs, culture media was replaced with fresh media and cells were treated with various concentration of DOX as shown in Fig. 4d. When cells were treated with free DOX without NAbs, a significant cytotoxicity was observed with the IC_{50} of 1.5 μM. However NAb pretreated cells when treated with DOX, significant reduction of toxicity related to DOX was observed. Whereas, in presence of minimum amount of DOX (0.01, 0.1, and 0.5 μM) the extent of toxicity was similar to that of free DOX, which is probably due to the additive effect exert by the presence of both DOX and NAb. On the other hand, at higher DOX concentration, owing to extreme toxic profile of DOX, significant toxic effect would expect, but such effect was delayed in the presence of nanoabsorbent. The reduction of DOX toxicity was due to the fact that the NAb absorbs DOX and depot into its core thereby minimizing the interaction of DOX with cellular organelles and microenvironment. In particular, the observed IC50 of DOX against B16-F10 melanoma has been shifted to 5μM in the presence of NAb. It is evident from our absorption and cellular studies that NAbs could hold promising detoxifying agents for smaller chemotherapeutics depending on the NAbs core and drug properties.

Conclusions

A biocompatible, biodegradable, and biomimetic NAbs as a cellular detoxifying agent was studied taking DOX as a model cationic drug. The interaction affinity between PLGA carboxylate terminated negatively charged nanoparticles when wrapped with RBC membranes, absorption of positively charged small molecule drug, DOX, was increased significantly. The interaction of DOX with NAb was found to be charge dependent as no or minimal interaction was observed when the negatively charged drug, MTX, was used for the absorption study. NAbs with its core shell structure and the surface properties of RBC offer the several advantages, including differential surface functionalization such as insertion of synthetic phospholipids other than RBC membrane and target specific ligand binding based on surface properties and capture molecules. Moreover, by optimizing the internal surface modification, NAbs could be an ideal platform for intoxication support.

Acknowledgements

The authors acknowledge the support from the Department of Chemistry and the Nanotechnology Innovative Center of Kansas State (NICKS), Kansas State University (KSU), Manhattan, Kansas. The authors also thank the Confocal Core supported by CVM-KSU.

Notes and references

1 V. T. DeVita and E. Chu, *Cancer Res.*, 2008, **68**, 8643–8653.
2 B. A. Chabner and T. G. Roberts, *Nat. Rev. Cancer*, 2005, **5**, 65–72.
3 B. Gustavsson, G. Carlsson, D. Machover, N. Petrelli, A. Roth, H.-J. Schmoll, K.-M. Tveit and F. Gibson, *Clin. Colorectal Cancer*, 2015, **14**, 1–10.
4 US6727253 B2, 2004.
5 K. Chatterjee, J. Zhang, N. Honbo and J. S. Karliner, *Cardiology*, 2010, **115**, 155–162.
6 M. Grissinger, *Pharm. Ther.*, 2009, **34**, 175–176.
7 E. Kassner, *J. Pediatr. Oncol. Nurs.*, 2000, **17**, 135–148.
8 A. Banerjee, T. M. Brotherston, B. G. Lamberty and R. C. Campbell, *Postgrad. Med. J.*, 1987, **63**, 5–9.
9 R. T. Dorr and D. S. Alberts, *Cancer Treat. Rep.*, 1981, **65**, 1001–1006.
10 K. L. Cumpston, S. E. Aks, T. Sigg and E. Pallasch, *J. Emerg. Med.*, 2010, **38**, 171–174.
11 J. C. Y. Lo, C. Ubaldo and F. L. Cantrell, *Clin. Toxicol. Phila. Pa*, 2012, **50**, 414–417.
12 Pillay, *Modern Medical Toxicology*, Jaypee Brothers Publishers, 2012.
13 J. W. Lee, *Electrolytes Blood Press. E BP*, 2010, **8**, 72–81.
14 B. Mokhlesi, J. B. Leikin, P. Murray and T. C. Corbridge, *Chest*, 2003, **123**, 897–922.
15 J. Stange, *Organogenesis*, 2011, **7**, 64–73.
16 J.-M. Saudubray, G. van den Berghe and J. H. Walter, *Inborn Metabolic Diseases: Diagnosis and Treatment*, Springer Science & Business Media, 2011.
17 A. Parés, L. Cisneros, J. M. Salmerón, L. Caballería, A. Mas, A. Torras and J. Rodés, *Am. J. Gastroenterol.*, 2004, **99**, 1105–1110.
18 S. Aula, S. Lakkireddy, K. Jamil, A. Kapley, A. V. N. Swamy and H. R. Lakkireddy, *RSC Adv.*, 2015, **5**, 47830–47859.
19 K. K. Awasthi, A. Awasthi, R. Verma, N. Kumar, P. Roy, K. Awasthi and P. J. John, *RSC Adv.*, 2015, **5**, 34927–34935.
20 J.-C. Leroux, *Nat. Nanotechnol.*, 2007, **2**, 679–684.
21 B. D. Henry, D. R. Neill, K. A. Becker, S. Gore, L. Bricio-Moreno, R. Ziobro, M. J. Edwards, K. Mühlemann, J. Steinmann, B. Kleuser, L. Japtok, M. Luginbühl, H. Wolfmeier, A. Scherag, E. Gulbins, A. Kadioglu, A. Draeger and E. B. Babiychuk, *Nat. Biotechnol.*, 2015, **33**, 81–88.
22 P. Aggarwal, J. B. Hall, C. B. McLeland, M. A. Dobrovolskaia and S. E. McNeil, *Adv. Drug Deliv. Rev.*, 2009, **61**, 428–437.
23 B. Howell and A. Chauhan, *J. Colloid Interface Sci.*, 2008, **319**, 81–93.
24 A. Sasidharan, J. E. Riviere and N. A. Monteiro-Riviere, *J. Mater. Chem. B*, 2015, **3**, 2075–2082.
25 F. D. Sahneh, C. M. Scoglio, N. A. Monteiro-Riviere and J. E. Riviere, *Nanomed.*, 2015, **10**, 25–33.
26 Z. Lin, N. A. Monteiro-Riviere and J. E. Riviere, *Wiley Interdiscip. Rev. Nanomed. Nanobiotechnol.*, 2015, **7**, 189–217.
27 M. Tanaka, A. Mochizuki, N. Ishii, T. Motomura and T. Hatakeyama, *Biomacromolecules*, 2002, **3**, 36–41.
28 C.-M. J. Hu, R. H. Fang, J. Copp, B. T. Luk and L. Zhang, *Nat. Nanotechnol.*, 2013, **8**, 336–340.

29 C.-M. J. Hu, L. Zhang, S. Aryal, C. Cheung, R. H. Fang and L. Zhang, *Proc. Natl. Acad. Sci.*, 2011, **108**, 10980–10985.
30 S. Aryal, C.-M. J. Hu, R. H. Fang, D. Dehaini, C. Carpenter, D.-E. Zhang and L. Zhang, *Nanomed.*, 2013, **8**, 1271–1280.